Clinical neuroanatomy

Altered functional connectivity in lesional peduncular hallucinosis with REM sleep behavior disorder

Maiya R. Geddes [a,b,*], *Yanmei Tie* [c], *John D.E. Gabrieli* [a],
Scott M. McGinnis [b], *Alexandra J. Golby* [c] *and Susan Whitfield-Gabrieli* [a]

[a] *Department of Brain and Cognitive Sciences and McGovern Institute for Brain Research, Massachusetts Institute of Technology, Cambridge, MA, USA*
[b] *Brigham and Women's Hospital, Division of Cognitive and Behavioral Neurology, Harvard Medical School, Boston, MA, USA*
[c] *Brigham and Women's Hospital, Department of Neurosurgery, Harvard Medical School, Boston, MA, USA*

ABSTRACT

Brainstem lesions causing peduncular hallucinosis (PH) produce vivid visual hallucinations occasionally accompanied by sleep disorders. Overlapping brainstem regions modulate visual pathways and REM sleep functions via gating of thalamocortical networks. A 66-year-old man with paroxysmal atrial fibrillation developed abrupt—onset complex visual hallucinations with preserved insight and violent dream enactment behavior. Brain MRI showed restricted diffusion in the left rostrodorsal pons suggestive of an acute ischemic stroke. REM sleep behavior disorder (RBD) was diagnosed on polysomnography. We investigated the integrity of ponto-geniculate-occipital circuits with seed-based resting-state functional connectivity MRI (rs-fcMRI) in this patient compared to 46 controls. Rs-fcMRI revealed significantly reduced functional connectivity between the lesion and lateral geniculate nuclei (LGN), and between LGN and visual association cortex compared to controls. Conversely, functional connectivity between brainstem and visual association cortex, and between visual association cortex and prefrontal cortex (PFC) was significantly increased in the patient. Focal damage to the rostrodorsal pons is sufficient to cause RBD and PH in humans, suggesting an overlapping mechanism in both syndromes. This lesion produced a pattern of altered functional connectivity consistent with disrupted visual cortex connectivity via de-afferentation of thalamocortical pathways.

* *Corresponding author.* Department of Brain and Cognitive Sciences and McGovern Institute for Brain Research, Massachusetts Institute of Technology, Cambridge, MA, USA.
E-mail addresses: mgeddes@mit.edu (M.R. Geddes), ytie@partners.org (Y. Tie), gabrieli@mit.edu (J.D.E. Gabrieli), sm93@partners.org (S.M. McGinnis), agolby@partners.org (A.J. Golby), swg@mit.edu (S. Whitfield-Gabrieli).

1. Introduction

In two seminal papers, Norman Geschwind outlined a disconnection framework for understanding the emergence of clinical syndromes from localized brain lesions (Geschwind, 1965). This work along with contemporary connectionist theories (Catani & ffytche, 2005) underscores the distributed network effects of focal brain injury (diaschisis). A hodotopic model of visual hallucinations emphasizes dysfunction localized within specific brain regions (topological) and aberrant connectivity between regions (hodological) (Catani & ffytche, 2005; ffytche, 2008). Advances in human brain imaging, in particular resting-state functional connectivity MRI (rs-fcMRI), allow for the direct testing of atypical functional connection in the living human brain.

Described by Lhermitte (1922), peduncular hallucinosis (PH) occurs with focal lesions of the brainstem or thalamus (Benke, 2006). Here, we present a case study of a patient with a brainstem stroke associated with new-onset PH and REM sleep behavior disorder (RBD). RBD and visual hallucinations are important non-motor features of neurodegenerative syn-ucleinopathies including Parkinson's disease (PD) and Lewy body dementia (LBD). The association of these syndromes secondary to a brainstem lesion suggests that they share a common underlying neural mechanism.

Theoretical 'release' of visual association cortex is used to explain many forms of visual hallucinations (Cogan, 1973; Jackson, 1879; Kinsbourne & Warrington, 1963; Lance, 1976; Manford & Andermann, 1998; West, 1962). PH is hypothesized to result from brainstem damage in regions that modulate the lateral geniculate nucleus (LGN) (Manford & Andermann, 1998). Overlapping brainstem nuclei control thalamic state shifts and coordinate REM sleep (McCarley, Benoit, & Barrionuevo, 1983; Manford & Andermann, 1998; Sherman, 2001). Manford and Andermann (1998) proposed that in addition to causing sleep disturbance, a brainstem lesion could produce complex visual hallucinations via thalamic inhibition by impairing LGN transmission and reducing the fidelity of retino−geniculate−occipital signaling.

We focused our analysis on visual association, rather than calcarine, cortex based on the results of intraoperative stimulation, functional neuroimaging, and primate anatomical studies (ffytche et al., 1998; Foerster, 1931; Penfield & Perot, 1963; Sincich, Park, Wohlgemuth, & Horton, 2004). During stimulation studies by Penfield and Perot (1963), electric current applied to primary visual cortex produced formless "visual flashes and coloured lights", whereas stimulation of visual association cortex caused "an experiential response". Functional neuroimaging evidence also supports a key role of extrastriate cortex in the generation of complex visual hallucinations (ffytche et al., 1998). Relatedly, LGN has anatomical connectivity to extrastriate regions (e.g., V5) (Sincich et al., 2004) and aberrant function of the retino-geniculate-extrastriate pathway may underlie certain types of visual hallucinations in PD (Diederich, Stebbins, Schiltz, & Goetz, 2014).

To investigate the distributed, polysynaptic network impacts of the patient's lesion, we applied an inferentially powerful combined lesional-functional imaging approach.

Based on the Manford and Andermann (1998) model, we anticipated that there would be reduced connectivity, a surrogate for thalamic de-afferentation, between left rostrodorsal pons and LGN, and also between LGN and visual association cortex. In addition, we hypothesized that disrupted thalamocortical circuitry facilitates emergence of experiential symptoms via aberrant visual network reorganization. To test this hypothesis, we examined whole-brain connectivity from visual association cortex in the patient compared to controls in order to identify brain regions with pathologically increased connectivity that might support the subjective experience of hallucinations.

2. Report of a case

A 66-year-old right-handed man with paroxysmal atrial fibrillation, hypertension, and dyslipidemia underwent laparoscopic gastric bypass surgery. Anticoagulation was discontinued prior to surgery. His perioperative course was complicated by a traumatic Foley catheter placement, blood loss with a nadir in hemoglobin of 7.6 g/dL requiring transfusion, and hypotension to 80/50 mmHg. On the first postoperative day he developed vivid, complex visual hallucinations and violent dream enactment behaviors (DEB) with nocturnal vocalizations. He remained completely lucid throughout his hospital course and responded appropriately to questions; he recognized that his hallucinations were not real. Structural brain MRI three days after the surgery showed restricted diffusion in the left rostrodorsal pons suggestive of an acute ischemic infarct (Fig. 1). There was no evidence of cortical infarction on initial or follow up neuroimaging.

The patient provided detailed descriptions of "visions and dreams": he perceived moving images of synchronized swimmers in colorful uniforms. He reported simple hallucinations of "shapes on the wall, and colors and people [that] changed". He experienced metamorphopsias (visual distortions): the floor appeared uneven, clocks and pictures on the wall were distorted and seemed to grow and shrink. He perceived pink and yellow-tinted elementary geometric shapes that morphed from squares to triangles and fluctuated in size. His visions occurred throughout the day, without diurnal variation or hypnogogic/hypnopompic onset. Emotional content of the visual imagery was mildly disturbing. The hallucinations improved and by the fourth postoperative day he saw only simple hallucinations that worsened at the end of the day; he described red moving dot photopsias, "squiggly lines", and brown puffs of smoke.

The patient did not have fluctuations in arousal or attention. He was consistently oriented to time and place, correctly spelled 'world' backwards and listed months of the year backwards. His digit span forward was seven, and backwards span was four. Speech was fluent without paraphasic errors or word finding difficulty. Repetition, comprehension and performance on the Boston naming test (Kaplan, Goodglass, & Weintraub, 1983) were intact. His writing was normal, without micrographia. Memory registration and recall were intact. The patient had normal praxis. Evaluation in neuro-ophthalmology showed intact visual acuity and correct identification of color plates with each eye separately. Visual fields
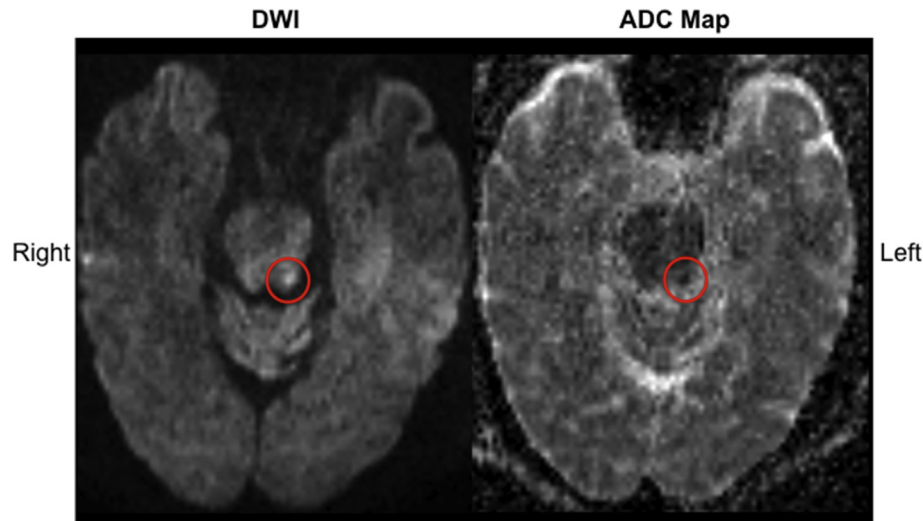
Fig. 1 − **Peduncular hallucinosis and REM sleep behavior disorder associated with ischemic pontine infarction. In the left rostrodorsal pons, diffusion-weighted imaging (DWI) shows high signal and apparent diffusion coefficient (ADC) map reveals low signal suggestive of an acute ischemic stroke.**

were normal on confrontation and Humphrey automated perimetry. Basic visuoperceptual function was also intact: he performed normally on the Benton visual form discrimination test (Benton, Sivan, Hamsher, Varney, & Spreen, 1994) and the Hooper visual organization test (Hooper, 1958).

At three-year follow up, the patient had persistent perceptual symptoms. He experienced multiple daily fleeting "shadows" in his peripheral vision in all lighting environments (*sensation de passage*); he had insight into the unreality of these hallucinations, but was unable to suppress a reflexive lateral saccade towards these apparitions when they occurred. He also reported visual misattributions (pareidolias). For example, he mistook fire hydrants for human forms but rapidly self-corrected his perceptual errors. In dim lighting, he experienced visual illusions with preserved insight. For example, he perceived "little insects" crawling over the carpet and "grasshoppers" on the toilet brush at night. The patient also reported difficulty tracking a golf ball after hitting it.

Serial comprehensive neurological examinations were unremarkable and unchanged at symptom onset and throughout 40 months of follow up. Cranial nerve exam was normal. In particular, visual fields were full on confrontation and there was no extinction to simultaneous visual stimuli. Range of eye movements was normal on saccades and smooth pursuit. Motor exam, sensation, reflexes, coordination and gait were normal. There was no retropulsion on pull testing. The patient did not have extrapyramidal signs: at 27 months post-stroke, he scored 2 (for diminished leg agility secondary to bilateral knee replacement) on the MDS unified Parkinson's disease rating scale (UPDRS), Part III (motor examination) (Movement Disorder Society Task Force, 2003). At 40-months, the patient's Hoehn and Yahr stage was zero (Hoehn & Yahr, 1967) and disability as measured by the modified Rankin scale (mRS) was 1 (out of 6) (Bonita & Beaglehole, 1988; Rankin, 1957).

Immediately after hospital discharge, the patient's spouse reported DEB during the second half of the night. While asleep, he inadvertently struck his wife and yelled profanities. At symptom onset, he had taken citalopram for three years to treat adjustment disorder; citalopram was discontinued in hospital. The patient had obstructive sleep apnea for over ten years and was compliant with continuous positive airway pressure (CPAP) therapy. Symptoms of sleepwalking, hypnogogic hallucinations, sleep paralysis, and cataplexy were absent. He reported daily bowel movements and lacked symptoms suggestive of autonomic dysfunction. DEB persisted and was refractory to treatment with melatonin 12 mg and clonazepam 2 mg. REM sleep without atonia (RSWA) was observed on two in-hospital polysomnography studies (Fig. 2)

Fig. 2 − **Patient polysomnography during REM sleep. There is persistent muscle activity in chin (musculus masseter) and leg (tibialis anterior) EMG leads during REM sleep indicative of REM sleep without atonia.**

consistent with a diagnosis of RBD. EEG did not show epileptiform activity.

3. Methods

3.1. Polysomnography and parasomnia diagnostic parameters

Long-term video-EEG polysomnography was performed in the hospital using a Polysmith Nihon Kohden system. The following parameters were used for documentation: 6 channel EEG (including C3 and C4 to mastoid); EOG (2 channels), respiration (nasal and oral thermistor, pulse oximeter, thoracic and abdominal respiratory inductance plethysmography, snore sensor and airflow measurement with pressure transducer airflow sensors), and bilateral EMGs of the musculus masseter and musculus tibialis anterior. A one-channel ECG was recorded. Polysomnography was performed under continuous observation by trained medical staff.

The patient showed RSWA during polysomnography (Fig. 2). RBD diagnosis was based on the presence of RSWA and DEB in the absence of EEG epileptiform abnormality during REM sleep in accordance with the International Classification of Sleep Disorders (2nd edition) (American Academy of Sleep Medicine, 2005). RSWA was defined as the presence of sustained tonic activity (increased chin EMG amplitude during greater than 50% of an epoch) and excessive phasic activity (at least 5, three-second epochs containing transient bursts of muscle activity) during a 30-s epoch of REM sleep.

3.2. Participants

The patient underwent rs-fcMRI 32 months after the onset of his symptoms. At this time his complex visual hallucinations had resolved, although, he experienced pareidolias, illusions in dim lighting, and approximately eight daily episodes of 'passage' hallucinations in his lateral visual field. The patient did not report perceptual events during the scanning session.

Resting-state functional connectivity MRI (rs-fcMRI) data were gathered in the patient and 27 Controls [15 women; age = 25.6 ± 5.0 years (mean ± SD)]. Participants were right-handed native English speakers. All volunteers had no history of neurological or psychiatric illness. To ensure our findings could not be accounted for by age effects, or differences in imaging acquisition parameters, an independent group of 16 healthy, age-matched right-handed Older Controls (8 women; age = 62.0 ± 10.9 years) was recruited from a separate institution. To control for potential changes in cerebral blood flow or functional connectivity previously reported in patients with obstructive sleep apnea (OSA) (Durgan & Bryan, 2012; Zhang et al., 2012), we recruited 3 right-handed OSA Controls (3 men; age = 58.0 ± 6.1 years). All OSA Controls had previously undergone diagnostic in-hospital polysomnography. Two of the OSA Controls were compliant with CPAP therapy and all endorsed at least three (of four) symptoms on the OSA STOP questionnaire (Chung et al., 2008).

All Older and OSA Controls scored at least 26/30 on the Montreal Cognitive Assessment (Nasreddine et al., 2005). All participants provided written, informed consent prior to participation in the study, in accordance with the Declaration of Helsinki. The Partners Institutional Review Board and the MIT committee on the use of humans as experimental subjects (COUHES) approved the study protocol.

3.3. MRI data acquisition

Functional magnetic resonance imaging (fMRI) data from the patient were acquired using a 3-T Siemens Magnetom Verio scanner (Siemens, Munich, Germany) paired with a 12-channel phased-array whole-head coil. Motion was reduced with foam pillows. T1-weighted magnetization-prepared rapid acquisition with gradient echo (MPRAGE) anatomical images were collected with the following parameters: time repetition (TR) = 1800 msec, time echo (TE) = 2.95 msec, flip angle (FA) = 12°, 160 slices, .78 × .78 × 1 mm resolution. Functional T2*-weighted images were gathered over two sessions of 5 min using echo-planar imaging (EPI) sensitive to blood oxygenation level-dependent (BOLD) contrast with the following parameters: TR = 2000 msec, TE = 30 msec, FA = 90°, 30 axial slices, ascending sequence, 3.44 × 3.44 × 4 mm resolution. The patient and controls were instructed to remain still and alert with eyes closed during the scanning. To allow for T1-equilibration effects, 10 dummy volumes were discarded prior to acquisition.

Imaging data from Controls were obtained using a 3 T GE Signa system (General Electric, Milwaukee, WI, USA). Whole brain T1-weighted axial 3D spoiled gradient recalled (SPGR) structural images were acquired using array spatial sensitivity encoding technique (ASSET, i.e., parallel imaging) and an 8-channel head coil (TR = 7.8 msec, TE = 3.0 msec, flip angle = 20°, 176 slices, .5 × 0.5 × 1 mm resolution). BOLD functional images were acquired over 7 min using single-shot gradient-echo EPI and a standard quadrature head coil (TR = 2000 msec, TE = 40 msec, FA = 90°, 27 axial slices, ascending sequence, 2 × 2 × 4 mm resolution).

FMRI data from Older Controls and OSA Controls were gathered using a 3-Tesla Siemens Tim Trio scanner paired with a 32-channel head coil. T1-weighted MPRAGE anatomical images were obtained: TR = 2530 msec, TE = 3.39 msec, FA = 7.0°, 176 slices, 1 mm isotropic resolution. Resting state T2*-weighted images were obtained with an ascending EPI sequence: TR = 2500 msec, TE = 30 msec, FA = 90°, 30 slices, 150 volumes, 6.5 min, 3.1 × 3.1 × 3.4 mm resolution.

3.4. Data preprocessing

Resting state data were preprocessed in SPM8 (Wellcome Department of Imaging Neuroscience, London, UK; http://www.fil.ion.ucl.ac.uk/spm). Pre-processing procedures included: (1) slice-timing correction; (2) rigid body motion correction by realigning all images to the first image of the functional run; (3) segmentation and normalization of the structural images to the Montreal Neurological Institute/International Consortium for Brain Mapping (MNI/ICBM) 152 template; (4) normalization of the functional images based on the structural normalization matrix; (5) artifact detection and rejection using the *art* tool (http://www.nitrc.org/projects/artifact_detect); and (6) spatial smoothing with an isotropic 6 mm full-width at half-maximum (FWHM) Gaussian kernel.

3.5. Analysis

Rs-fcMRI analysis was performed using a seed-based approach with in-house, custom software 'Conn toolbox' (http://www.nitrc.org/projects/conn) (Whitfield-Gabrieli & Nieto-Castanon, 2012). Physiological and other sources of noise were estimated using the aCompcor method (Behzadi, Restom, Liau, & Liu, 2007) and regressed out together with movement-related and artifactual covariates. The residual BOLD time series was band-pass filtered (.009−.08 Hz) and linearly detrended.

To examine brainstem−geniculate, geniculate−occipital and brainstem−occipital functional connectivity, we performed ROI-to-ROI analyses using *a priori* anatomically defined regions-of-interest. To determine the specificity of our findings, we compared the functional connectivity of the focal lesion in the left rostrodorsal pons to its right non-lesioned homologue. Left and right pontine ROI were drawn by an expert rater on the patient's T1-weighted structural image in *fslview*, and normalized to the MNI standard brain (Fig. 3A). To ensure that the lesioned left rostrodorsal pons was comprised of functional neural tissue, we compared the time-series signal-to-noise ratio (tSNR) in left and right rostrodorsal pontine ROI in the patient versus controls. TSNR from these seeds was calculated as the ratio of mean SNR over the time-series standard deviation from pre-processed EPI data (Triantafyllou, Polimeni, & Wald, 2011).

The bilateral lateral occipital cortices ROI was generated by FreeSurfer segmentation of the MNI/ICBM 152 template (Fig. 3B). The bilateral lateral geniculate nuclei (LGN) ROI was based on a functional anatomical study where flickering checkerboard stimuli were used to identify mean peak activations in right and left LGN across nine healthy participants (Kastner et al., 2004). We generated 5 mm radius spheres around these peak functional coordinates to define the LGN ROI [MNI x, y, z: 23, −21, −10 (right); −22, −22, −10 (left)] (Fig. 3B).

First-level correlation maps were obtained by extracting the residual BOLD time course from each ROI and calculating Pearson's correlation coefficients between this time course and the time course of all other brain voxels. Correlation coefficients were Fisher transformed to 'z' scores to increase normality prior to second-level General Linear Model analyses. We interrogated each ROI by extracting the mean z-value for all participants. We applied single-case methodology developed by Crawford and Howell (1998) to test for significant functional connectivity differences in mean z-values between the patient and controls. To control for potential OSA-related confounds in the patient, we assessed functional connectivity in the three OSA Controls compared to all other controls using the non-parametric Mann−Whitney test. Significance was set at $p < .05$, two-tailed.

To identify brain regions with paradoxically increased coupling to lateral occipital cortex in the patient greater than controls, we performed an exploratory seed-to-voxel analysis, corrected for multiple comparisons. We tested for differences (patient *vs* controls) by performing a whole-brain seed-to-voxel analysis using a two-sample t-test. Clusters were significant at a false discovery rate (FDR) cluster-corrected threshold of $p < .05$. We interrogated the resulting significant cluster qualitatively by extracting the mean z-value for all participants.

4. Results

The patient had minimal mean movement in all directions ($x = .016$ mm; $y = .118$ mm; $z = .099$ mm; pitch = .052 degrees;
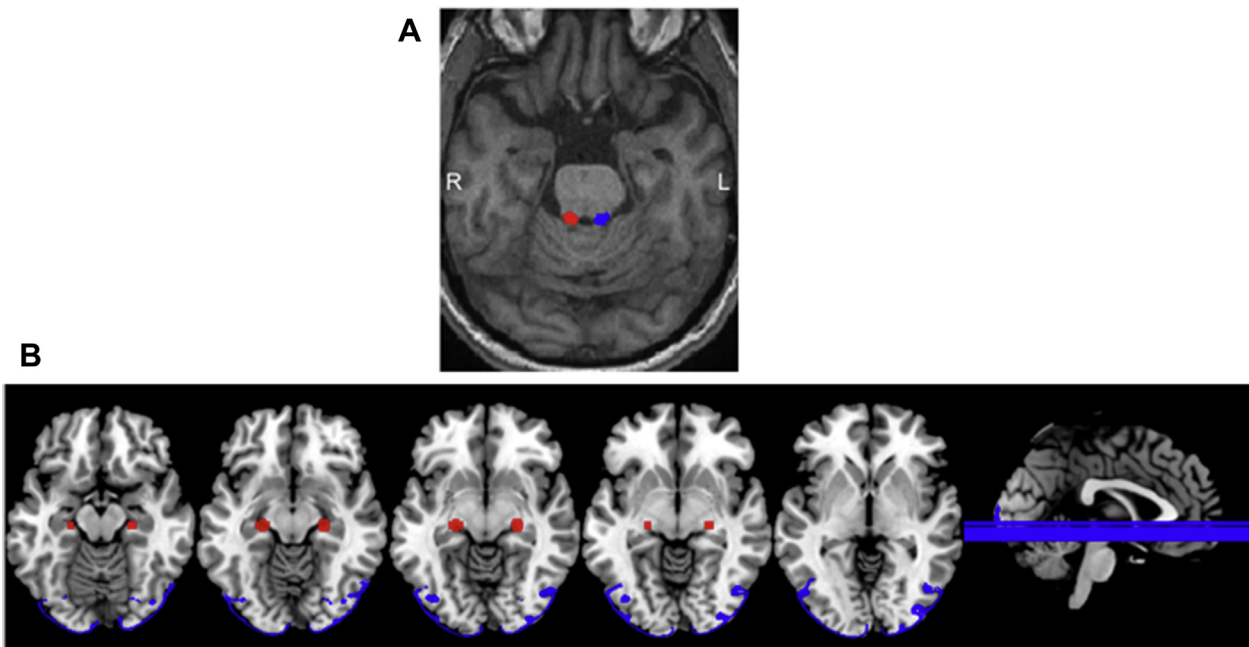

Fig. 3 − *A priori* regions of interest (ROIs). (A) Left (blue) and right (red) rostrodorsal pontine ROI displayed on an axial T1-weighted image of the patient's brainstem. (B) Bilateral lateral geniculate nuclei ROI (red) and lateral occipital cortices ROI (blue).

roll = .012 degrees; yaw = .023 degrees) and no scan-to-scan movement outliers over 2 mm. Despite diversity in imaging acquisition parameters, we identified consistent functional connectivity differences between the patient and Controls, and the patient and Older Controls. Thus, our findings cannot be explained by potential differences in SNR. Similarity and reliability of rs-fcMRI results across different scanners and acquisition parameters have been shown previously (Jann et al., 2015; Van Dijk et al., 2010). There was no significant difference in tSNR between right (non-lesioned) and left (remotely lesioned) rostrodorsal pons in the patient versus controls supporting the functionality of neural tissue at the site of the remote stroke (right vs left difference: patient 3.1, controls 2.3 ± 23.4; Crawford significance test, $t = .2$, $p = .8$).

Unlike controls, the patient displayed a positive correlation between the left pontine ROI and lateral occipital cortices [Older Controls mean z-value −.023 (SD .07); Controls mean z-value −.017 (SD .06); patient z-value .192]. To test for a difference in functional connectivity, we conducted a two-tailed Crawford single-case significance test that accounts for control sample size (Crawford & Howell, 1998). This revealed a significant increase in functional connectivity between the left rostrodorsal pons and the lateral occipital cortices in the patient compared to Controls ($t = 3.5$, $p = .002$); an identical analysis also showed significantly enhanced functional connectivity in the patient compared to Older Controls ($t = 3.0$, $p = .008$) (Fig. 4).

To test for disruption in brainstem-geniculate connectivity, we again applied the Crawford test to the mean z-values extracted from the left rostrodorsal pons to LGN ROI [Older Controls mean z-value .004 (SD .08); Controls mean z-value .072 (SD .09); patient z-value −.26]. This revealed significantly decreased functional connectivity between left rostrodorsal pons and LGN in the patient versus Controls ($t = 3.5$, $p = .002$) and between the patient and Older Controls ($t = 3.3$, $p = .005$) (Fig. 4). Critically, there was also significantly decreased geniculate-occipital functional connectivity in the patient compared to Controls ($t = 2.9$, $p = .007$) and Older Controls ($t = 2.5$, $p = .023$) [Older Controls mean z-value .004 (SD .07); Controls mean z-value −.002 (SD .06); patient z-value −.183] (Fig. 4). Two exploratory, whole-brain seed-to-voxel analyses from left rostrodorsal pons and LGN demonstrated similar findings (see Supplemental Materials).

To assess the specificity of the left pontine connectivity findings, we performed identical functional connectivity analyses from the right, non-lesioned rostrodorsal pontine ROI. There was no difference in right pontine to LGN functional connectivity in the patient versus controls [Older Controls mean z-value .036 (SD .08); Controls mean z-value .067 (SD .1); patient z-value-.02; all $p > .38$]. Similarly, there was no difference in right pons to lateral occipital functional connectivity in the patient compared to controls [Older Controls mean z-value −.015 (SD .08); Controls mean z-value −.007 (SD .07); patient z-value .036; all $p > .53$]. In addition, controls showed no difference between left versus right rostrodorsal pons to LGN connectivity (two-sample t-test, $t = .2$, $p = .8$) and no difference in left versus right rostrodorsal pons to lateral occipital connectivity (two-sample t-test, $t = .4$, $p = .7$).
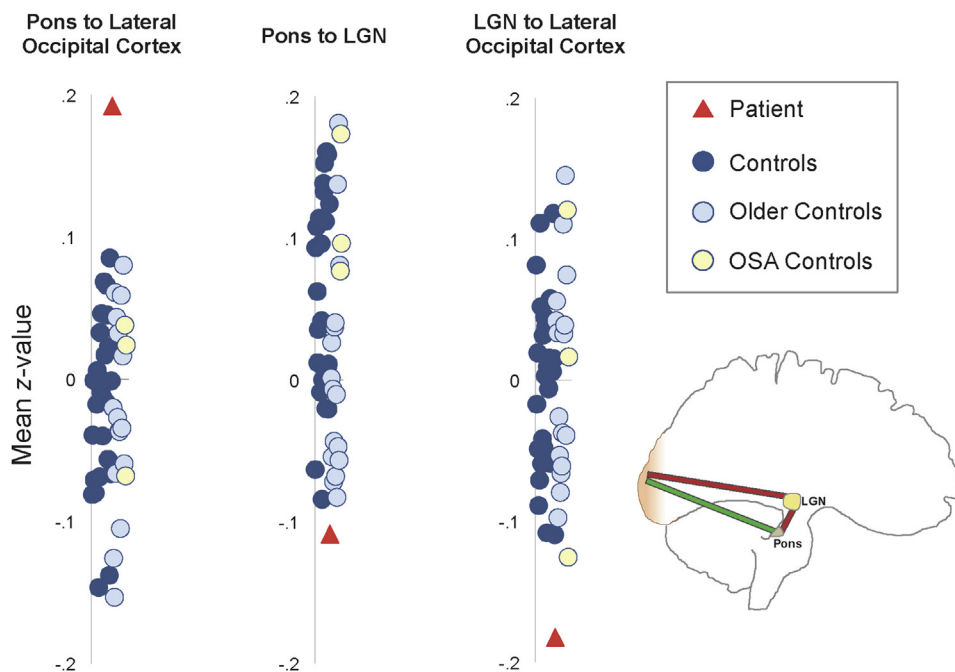

Fig. 4 − Dissociated patterns of functional connectivity in the ponto-geniculate-occipital system in the patient versus controls. There is significantly increased resting-state functional connectivity between left rostrodorsal pons and lateral occipital ROI in the patient compared to controls. Conversely, the patient shows significantly reduced functional connectivity between left rostrodorsal pons and lateral geniculate nuclei (LGN), and also between LGN and lateral occipital cortices. Obstructive sleep apnea (OSA) Controls do not show significant differences in functional connectivity compared to all other controls. The schematic diagram (bottom right) depicts the change in functional connectivity between the ROIs in the patient compared to controls (red = reduction; green = augmentation).

The patient's pattern of functional connectivity did not resemble that of the OSA Controls, suggesting that our findings are not confounded by comorbid OSA in the patient (Fig. 4). There was no significant difference in ponto–geniculate–occipital functional connectivity in OSA Controls compared to all other controls (Mann–Whitney, ponto-occipital: $U = 54.0$, $p = .6$; ponto–geniculate: $U = 35.0$, $p = .2$; geniculate–occipital: $U = 61.0$, $p = .9$).

An exploratory, whole-brain seed-to-voxel analysis, corrected for multiple comparisons, showed significantly increased functional connectivity in the patient versus controls between the lateral occipital ROI and two clusters within prefrontal cortex (PFC) (Fig. 5). The largest cluster was located in left orbitofrontal cortex (OFC) (peak MNI x, y, z coordinates: -18, 16, -12; spatial extent: 633 voxels; $p = .03$, cluster-level, FDR-corrected). A second cluster was identified in bilateral supplementary eye field (SEF) and supplementary motor area (SMA) (peak MNI x, y, z coordinates: 2, -8, 76; spatial extent: 547 voxels; $p = .03$, cluster-level, FDR-corrected).

5. Discussion

We present a patient with acute-onset PH and RBD associated with a left rostrodorsal pontine ischemic stroke. We applied combined lesional and resting-state fMRI methodology to examine the distributed network effects of the patient's brainstem lesion in the chronic stage. We found significantly decreased functional connectivity between left rostrodorsal pons and LGN, and between LGN and visual association cortices in the patient compared to controls. In contrast, functional connectivity was significantly enhanced between visual association cortices and left rostrodorsal pons, and between visual association cortices and PFC in the patient versus controls. This case highlights a putative shared neural

substrate underlying visual hallucinations and RBD, two syndromes that commonly coexist in neurodegenerative alpha-synucleinopathies that involve brainstem synuclein deposition and degeneration.

Our patient had focal damage to rostrodorsal pons, encompassing multiple nuclei including locus coeruleus (LC), ventrolateral periaqueductal gray matter (vlPAG), and lateral pontine tegmentum (LPT) (Boeve et al., 2007). These brainstem regions modulate arousal and attention, REM behavioral state switching, and thalamocortical excitability (Boeve et al., 2007; Lu, Sherman, Devor, & Saper, 2006; Rogawski & Aghajanian, 1980; Sara, 2009). Disruption of these processes may underlie coexistent RBD and PH in this patient. In rodents, LC sends inhibitory noradrenergic inputs to visual cortex that improve perceptual acuity by gating target neurons (Hurley, Devilbiss, & Waterhouse, 2004; Sara, 2009). The patient had paradoxically augmented coupling between pons and visual association cortex. This could reflect dysfunctional "gain modulation" of LC on visual cortex, shifting the probability of spontaneous oscillations and integrative properties of cortical neurons (Haider, Duque, Hasenstaub, Yu, & McCormick, 2007; Sara & Bouret, 2012). Nonvisual brainstem regions (including vlPAG and LC) also project to LGN and thalamic reticular nucleus (Mackay-Sim, Sefton, & Martin, 1983; Rogawski & Aghajanian, 1980). The patient's diminished LGN functional connectivity may reflect disruption of thalamocortical loops and altered firing of inhibitory interneurons within LGN itself (Sherman & Guillery, 2001). Thus, a lesion in the vicinity of LC may alter tuning of retino–geniculate–occipital circuits and simultaneously influence sleep and visual pathways.

Related to our main finding, Purkinje hallucinations are associated with diminished connectivity between LGN and cortex accompanied by increased occipito-temporal connectivity (ffytche, 2008). A putative mechanism for this dissociation is a shift in the mode of thalamocortical firing from tonic
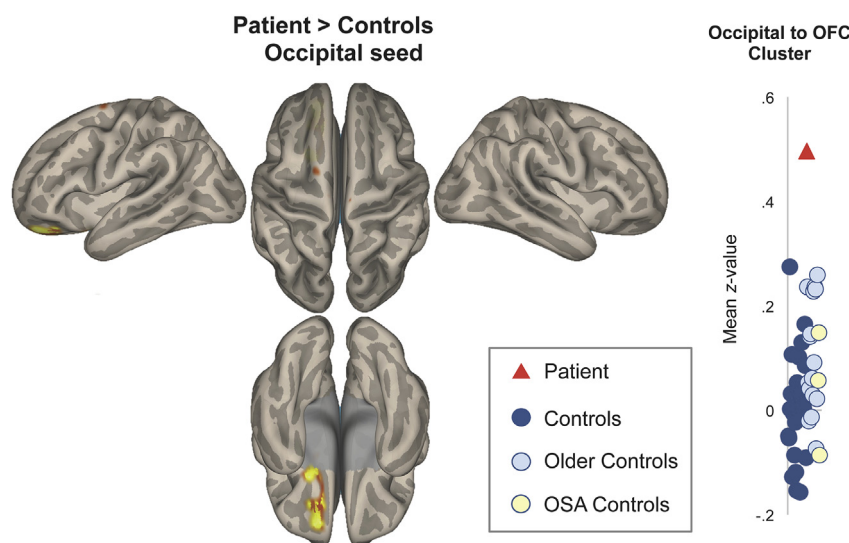

Fig. 5 – Increased functional connectivity between lateral occipital and prefrontal cortices in the patient versus controls. This exploratory, cluster-corrected seed-to-voxel analysis revealed significantly increased coupling between bilateral lateral occipital cortices and left orbitofrontal cortex (OFC), and between lateral occipital cortices and supplementary eye field in the patient. The mean z-value extracted from the OFC cluster is shown in the graph and is greater in the patient than the controls.

(where retinal inputs are accurately transmitted to cortex) to burst mode (where there is non-linear summation of retinal inputs in visual cortex) (ffytche, 2008; Sherman, 2001). Burst mode is induced by thalamic de-afferentation and is associated with diminished thalamic and increased cortical metabolic demand (Linás, Ribary, Jeanmonod, Kronberg, & Mitra, 1999). This mechanism may also underlie an array of positive symptoms in neurological/neuropsychiatric conditions, termed 'thalamocortical dysrhythmias' (ffytche, 2008; Jeanmonod, Magnin, & Morel, 1996; Llinás et al., 1999).

Hallucinations and illusions fall along a continuum: although this patient's well formed visual hallucinations resolved, he reported persistent visual illusions, pareidolias and 'passage' hallucinations. RBD, visual misperceptions and hallucinations are important non-motor features of neurodegenerative synucleinopathies including PD and LBD (Onofrj et al., 2013; Shine et al., 2014; Uchiyama et al., 2012). The coexistence of these syndromes secondary to a pontine lesion suggests a shared underlying neural mechanism. Convergent evidence suggests that brainstem alpha-synuclein deposition in LBD and PD contributes to development of visual hallucinations (Manford & Andermann, 1998; Onofrj et al., 2013). Relatedly, RBD in PD or LBD is associated with a lower Braak stage and independently predicts the development of hallucinations (Arnulf, 2013; Dugger et al., 2012). In the early stages of PD 20–45% of patients report fleeting sideway shadows ('passage' hallucinations) or a sensation of presence (Fénelon, Soulas, Cleret de Langavant, Trinkler, & Bachoud-Levi, 2011; Fénelon, Soulas, Zenasni, & de Langavant, 2010; Mack et al., 2012). Pareidolias and visual hallucinations are common in patients with LBD (Uchiyama et al., 2012). Patients with PD and visual hallucinations also show altered functional connectivity in attentional networks and structural changes in visuoperceptual pathways (Goldman et al., 2014; Shine et al., 2014). Based on the findings in this patient, we hypothesize that altered functional connectivity in PD patients with hallucinations may occur via altered LC inputs to attentional networks. This hypothesis is consistent with human fMRI and EEG data that show coupling between LC and the ventral attention network (Walz et al., 2013).

The patient showed increased functional connectivity between visual association cortex and left orbitofrontal cortex (OFC), a region that plays an important role in top-down visual processing. The patient's pareidolias might be explained in light of this finding. OFC is key in generating expectations about image content (Bar et al., 2006) and signal propagation from OFC to visual cortex facilitates object recognition (Bar et al., 2006; O'Shea & Walsh, 2006; Petrides, Alivisatos, & Frey, 2002; Trapp & Bar, 2015). Aberrant OFC to visual association cortex connectivity could impede the mapping of internally generated predictions onto incoming visual information and impair rapid processing of ambiguous visual stimuli. OFC is structurally connected to occipital cortex via the inferior fronto-occipital fasciculus (IFOF) (Forkel et al., 2014). Altered structural integrity of IFOF is associated with visual hallucinations in schizophrenia (Amad et al., 2014; Ćurčić-Blake et al., 2015). Relatedly, intraoperative stimulation of PFC produces visual hallucinations (Vignal, Chauvel, & Halgren, 2000) and frontal leucotomy can improve or abolish visual hallucinations (McLardy & Meyer, 1949).

The patient also demonstrated enhanced functional connectivity between visual association cortex and supplementary eye field (SEF). SEF is a region at the pre-SMA/SMA boarder with extensive PFC connectivity that supplies second-order neurons to middle temporal area (MT) of the dorsal visual stream (Grosbras, Lobel, Van de Moortele, LeBihan, & Berthoz, 1999; Ninomiya, Sawamura, Inoue, & Takada, 2012; Tehovnik, Sommer, Chou, Slocum, & Schiller, 2000). SEF is associated with executive control of saccades, motion perception and monitoring of visual search (Purcell, Weigan, & Schall, 2012). During kinematic stimulation, PD patient with visual hallucinations show hyperactivation of SEF (Stebbins et al., 2004). Diederich et al. (2014) hypothesized that deficient corollary discharges to the frontal eye field and reduced integrity of the retino−geniculate−extrastriate (MT/V5) system cause 'passage' hallucinations in PD. We propose that a similar mechanism underlies the passage hallucinations reported by the patient.

Although sleep disturbances are common in PH (Manford & Andermann, 1998), to our knowledge coexistent RBD and PH were reported in only one prior case (Vetrugno et al., 2009) in whom SPECT revealed hyperperfusion in lateral occipital cortex and PFC during visual hallucinations, similar to our findings. There are a handful of lesional RBD cases secondary to multiple sclerosis, vascular malformation, stroke, and cerebral vasculitis (Boeve et al., 2007; Iranzo & Aparicio, 2009; St Louis et al., 2014). Lesional studies in rodents and humans suggest that mutually inhibitory 'REM on' and 'REM off' brainstem systems regulate sleep states (Lu et al., 2006). Our patient's rostrodorsal pontine lesion putatively encapsulates key 'REM off' brainstem regions including LPT, vlPAG, and LC (Boeve et al., 2007). In rodents, vlPAG and LPT receive excitatory noradrenergic projections from LC, and lesions to these regions increase the amount of REM sleep (Lu et al., 2006). Although LC is quiescent during REM sleep, patients with PD and RBD show reduced structural integrity of LC (Garcia-Lorenzo et al., 2013). It is controversial whether visual hallucinations in PD represent REM intrusions during wakefulness (Arnulf, 2013; Arnulf et al., 2000; Manni et al., 2011; Nomura et al., 2003).

One potential concern is the use of a stroke site as a region of interest. However, certain features of this case justify the use of the left pontine ROI: the brainstem lesion was small, chronic, and showed no residual T2-weighted changes on structural imaging. Critically, there was a high time-series signal-to-noise ratio (tSNR) within the lesion and no difference in tSNR in the left (lesioned) compared to the right (non-lesioned) rostrodorsal pons. Based on this finding, and given the patient's persistent symptoms, we hypothesize that the left rostrodorsal pontine lesion encompasses dysfunctional rather than non-functional neural tissue. The lack of connectivity changes from the right pontine ROI support the specificity of our findings.

In summary, this study supports the application of rs-fcMRI to characterize the distributed network impacts of focal brain injury in individuals. We identified a pattern of altered functional connectivity suggestive of thalamic de-afferentation and reorganization of the visual network secondary to rostrodorsal pontine damage. This case enhances our understanding of brainstem modulation of

geniculate–occipital pathways. Our approach may help identify novel, individualized therapeutic cortical targets for non-invasive neurostimulation.

Acknowledgments

Supplementary data

Supplementary data related to this article can be found at http://dx.doi.org/10.1016/j.cortex.2015.10.015.

R E F E R E N C E S

Amad, A., Cachia, A., Gorwood, P., Pins, D., Delmaire, C., Rolland, B., et al. (2014). The multimodal connectivity of the hippocampal complex in auditory and visual hallucinations. *Molecular Psychiatry, 19*, 184–191.

American Academy of Sleep Medicine. (2005). *International classification of sleep disorders: Diagnostic and coding manual* (2nd ed.). Rochester, MN: Sleep Disorders Association (ICSD-2).

Arnulf, I. (2013). Dream imagery, rapid eye movement sleep behavior disorder, and hallucinations. *Sleep and Biological Rhythms, 11*, 15–20.

Arnulf, I., Bonnet, J. P., Damier, P., Bejjani, B. P., Seilhean, D., Derenne, J. P., et al. (2000). Hallucinations, REM sleep, and Parkinson's disease: a medical hypothesis. *Neurology, 55*(2), 281–288.

Bar, M., Kassam, K. S., Ghuman, A. S., Boshyan, J., Schmid, A. M., Dale, A. M., et al. (2006). Top-down facilitation of visual recognition. *PNAS, 103*(2), 449–454.

Behzadi, Y., Restom, K., Liau, J., & Liu, T. T. (2007). A component based noise correction method (CompCor) for BOLD and perfusion based fMRI. *NeuroImage, 37*, 90–101.

Benke, T. (2006). Peduncular hallucinosis: a syndrome of impaired reality monitoring. *Journal of Neurology, 253*(12), 1561–1571.

Benton, A. L., Sivan, A. B., Hamsher, K., Varney, N. R., & Spreen, O. (1994). *Contributions to neuropsychological assessment: A clinical manual* (2nd ed.). New York: Oxford University Press.

Boeve, B. F., Silber, M. H., Saper, C. B., Ferman, T. J., Dickson, D. W., Parisi, J. E., et al. (2007). Pathophysiology of REM sleep behaviour disorder and relevance to neurodegenerative disease. *Brain, 130*(11), 2770–2788.

Bonita, R., & Beaglehole, R. (1988). Modification of Rankin Scale: recovery of motor function after stroke. *Stroke, 19*(12), 1497–1500.

Catani, M., & ffytche, D. H. (2005). The rises and falls of disconnection syndromes. *Brain, 128*(10), 2224–2239.

Chung, F., Yegneswaran, B., Liao, P., Chung, S. A., Vairavanathan, S., Islam, S., et al. (2008). STOP Questionnaire: a tool to screen patients for obstructive sleep apnea. *Anesthesiology, 108*(5), 812–821.

Cogan, D. G. (1973). Visual hallucinations as release phenomena. *Graefe's Archive for Clinical and Experimental Ophthalmology, 188*, 139–150.

Crawford, J. R., & Howell, D. C. (1998). Comparing an individual's test score against norms derived from small samples. *The Clinical Neuropsychologist, 12*, 482–486.

Ćurčić-Blake, B., Nanetti, L., van der Meer, L., Cerliani, L., Renken, R., Pijnenborg, G. H. M., et al. (2015). Not on speaking terms: hallucinations and structural network disconnectivity in schizophrenia. *Brain Structure and Function, 220*, 407–418.

Diederich, N. J., Stebbins, G., Schiltz, C., & Goetz, C. G. (2014). Are patients with Parkinson's disease blind to blindsight? *Brain, 137*, 1838–1849.

Dugger, B. N., Boeve, B. F., Murray, M. E., Parisi, J. E., Fujishiro, H., Dickson, D. W., et al. (2012). Rapid eye movement sleep behavior disorder and subtypes in autopsy-confirmed dementia with Lewy bodies. *Movement Disorders, 27*(1), 72–78.

Durgan, D. J., & Bryan, R. M. (2012). Cerebrovascular consequences of obstructive sleep apnea. *Journal of the American Medical Association, 1*(4), e000091.

Fénelon, G., Soulas, T., Cleret de Langavant, L., Trinkler, I., & Bachoud-Levi, A. C. (2011). Feeling of presence in Parkinson's disease. *Journal of Neurology, Neurosurgery, and Psychiatry, 82*(11), 1219–1224.

Fénelon, G., Soulas, T., Zenasni, F., & de Langavant, L. C. (2010). The changing face of Parkinson's disease-associated psychosis: a cross-sectional study based on the new NINDS-NIMH criteria. *Movement Disorders, 25*, 755–759.

ffytche, D. H. (2008). The hodology of hallucinations. *Cortex, 44*, 1067–1083.

ffytche, D. H., Howard, R. J., Brammer, M. J., David, A., Woodruff, P., & Williams, S. (1998). The anatomy of conscious vision: an fMRI study of visual hallucinations. *Nature Neuroscience, 1*(8), 738–742.

Foerster, O. (1931). *The cerebral cortex in man* (pp. 309–312). Lancet, ii.

Forkel, S. J., de Schotten, M. T., Kawadler, J. M., Dell'Acqua, F., Danek, A., & Catani, M. (2014). The anatomy of fronto-occipital connections from early blunt dissections to contemporary tractography. *Cortex, 56*, 73–84.

Garcia-Lorenzo, D., Longo-Dos Santos, C., Ewenczyk, C., Leu-Semenescu, S., Gallea, C., Quattrocchi, G., et al. (2013). The coeruleus/subcoeruleus complex in rapid eye movement sleep behaviour disorders in Parkinson's disease. *Brain, 136*(7), 2120–2129.

Geschwind, N. (1965). Disconnexion syndromes in animals and man. *Brain, 88*, 237–294.

Goldman, J. G., Stebbins, G. T., Dinh, V., Bernard, B., Merkitch, D., deToledo-Morrell, L., et al. (2014). Visuoperceptive region atrophy independent of cognitive status in patients with Parkinson's disease with hallucinations. *Brain, 137*(Pt 3), 849–859.

Grosbras, M. H., Lobel, E., Van de Moortele, P. F., LeBihan, D., & Berthoz, A. (1999). An anatomical landmark for the supplementary eye fields in human revealed with functional magnetic resonance imaging. *Cerebral Cortex, 9*, 705–711.

Haider, B., Duque, A., Hasenstaub, A. R., Yu, Y., & McCormick, D. A. (2007). Enhancement of visual responsiveness by spontaneous local network activity in vivo. *Journal of Neurophysiology, 97*, 4186–4202.

Hoehn, M. M., & Yahr, M. D. (1967). Parkinsonism: onset, progression and mortality. *Neurology, 17*, 427–442.

Hooper, H. E. (1958). *The Hooper visual organization test: Manual.* Los Angeles: Western Pscyhologival Service.

Hurley, L. M., Devilbiss, D. M., & Waterhouse, B. D. (2004). A matter of focus: monoaminergic modulation of stimulus coding in mammalian sensory networks. *Current Opinion in Neurobiology, 14*(4), 488–495.

Iranzo, A., & Aparicio, J. (2009). A lesson from anatomy: focal brain lesions causing REM sleep behavior disorder. *Sleep Medicine, 10*(1), 9—12.

Jackson, J. H. (1879). Lectures on the diagnosis of epilepsy, Lecture III. *Medical Times and Gazette, 1*, 141—143.

Jann, K., Gee, D. G., Kilroy, E., Schwab, S., Smith, R. X., Cannon, T. D., et al. (2015). Functional connectivity in BOLD and CBF data: similarity and reliability of resting brain networks. *NeuroImage, 106*, 111—122.

Jeanmonod, D., Magnin, M., & Morel, A. (1996). j Low-threshold calcium spike bursts in the human thalamus. Common physiopathology for sensory, motor and limbic positive symptoms. *Brain, 199*, 363—375.

Kaplan, E. F., Goodglass, H., & Weintraub, S. (1983). *The Boston naming test* (Experimental edition). Philadelphia: Lea & Febiger.

Kastner, S., O'Connor, D. H., Fukui, M. M., Fehd, H. M., Herwig, U., & Pinsk, M. A. (2004). Funcitonal imaging of the human lateral geniculate nucleus and pulvinar. *Journal of Neurophysiology, 91*, 438—448.

Kinsbourne, M., & Warrington, E. K. (1963). A study of visual perseveration. *Journal of Neurology, Neurosurgery, and Psychiatry, 26*, 468—475.

Lance, J. W. (1976). Simple formed hallucinations confined to the area of a specific visual field defect. *Brain, 99*, 719—734.

Lhermitte, J. (1922). Syndrome de la calotte du pedoncule cerebral. Le troubles psycho-sensoriels dans les lesions due mesocephale. *Revista de Neurología, 2*, 1359—1365.

Linás, R. R., Ribary, U., Jeanmonod, D., Kronberg, E., & Mitra, P. P. (1999). Thalamocortical dysthythmia: a neurological and neuropsychiatric syndrome characterised by magnetoencephalograpy. *PNAS, 96*, 15222—15227.

Lu, J., Sherman, D., Devor, M., & Saper, C. B. (2006). A putative flip-flop switch for control of REM sleep. *Nature, 441*(7093), 589—594.

Mackay-Sim, A., Sefton, J., & Martin, P. R. (1983). Subcortical projections to lateral geniculate and thalamic reticular nuclei in the hooded rat. *The Journal of Comparative Neurology, 213*, 24—35.

Mack, J., Rabins, P., Anderson, K., Goldstein, S., Grill, S., Hirsch, E. S., et al. (2012). Prevalence of psychotic symptoms in a community-based parkinson disease sample. *American Journal of Geriatric Psychiatry, 20*(2), 123—132.

Manford, M., & Andermann, F. (1998). Complex visual hallucinations clinical and neurobiological insights. *Brain, 121*, 1819—1840.

Manni, R., Terzaghi, M., Ratti, P. L., Repetto, A., Zangaglia, R., & Pacchetti, C. (2011). Hallucinations and REM sleep behaviour disorder in Parkinson's disease: dream imagery intrusions and other hypotheses. *Consciousness and Cognition, 20*(4), 1021—1026.

McCarley, R. W., Benoit, O., & Barrionuevo, G. (1983). Lateral geniculate nucleus unitary discharge in sleep and waking: state- and rate-specific aspects. *Journal of Neurophysiology, 50*, 798—818.

McLardy, T., & Meyer, A. (1949). Anatomical correlates of improvement after leucotomy. *Journal of Mental Science, 95*, 182—196.

Movement Disorder Society Task Force on Rating Scales for Parkinson's Disease. (2003). The Unified Parkinson's Disease Rating Scale (UPDRS): status and recommendations. *Movement Disorders, 18*(7), 738—750.

Nasreddine, Z. S., Phillips, N. A., Bedirian, V., Charbonneau, S., Whitehead, V., Collin, I., et al. (2005). The Montreal Cognitive Assessment, MoCA: a brief screening tool for mild cognitive impairment. *Journal of the American Geriatrics Society, 53*(4), 695—699.

Ninomiya, T., Sawamura, H., Inoue, K., & Takada, M. (2012). Segregated pathways carrying frontally derived top-down signals to visual areas MT and V4 in macaques. *Journal of Neuroscience, 32*(20), 6851—6858.

Nomura, T., Inoue, Y., Mitani, H., Kawahara, R., Miyake, M., & Nakashima, K. (2003). Visual hallucinations as REM sleep behavior disorders in patients with Parkinson's disease. *Movement Disorders, 18*(7), 812—817.

Onofrj, M., Taylor, J. P., Monaco, D., Franciotti, R., Anzellotti, F., Bonanni, L., et al. (2013). Visual hallucinations in PD and Lewy body dementias: old and new hypotheses. *Behavioural Neurology, 27*(4), 479—493.

O'Shea, J., & Walsh, V. (2006). Trickle-down theories of vision. *Current Biology, 16*, R206—R209.

Penfield, W., & Perot, P. (1963). The brain's record of auditory and visual experiences: a final summary and discussion. *Brain, 86*, 595—696.

Petrides, M., Alivisatos, B., & Frey, S. (2002). Differential activation of the human orbital, mid-ventrolateral, and mid-dorsolateral prefrontal cortex during the processing of visual stimuli. *99*(8), 5649—5654.

Purcell, B. A., Weigan, P. K., & Schall, J. D. (2012). Supplementary eye field during visual search: salience, cognitive control, and performance monitoring. *Journal of Neuroscience, 32*(30), 10273—10285.

Rankin, J. (1957). Cerebral vascular accidents in patients over the age of 60. *Scottish Medical Journal, 2*(5), 200—215.

Rogawski, M. A., & Aghajanian, G. K. (1980). Modulation of lateral geniculate neurone excitability by noradrenaline microiontophoresis or locus coeruleus stimulation. *Nature, 287*, 731—734.

Sara, S. J. (2009). The locus coeruleus and noradrenergic modulation of cognition. *Nature Reviews Neuroscience, 10*(3), 211—223.

Sara, S. J., & Bouret, S. (2012). Orienting and reorienting: the locus coeruleus mediates cognition through arousal. *Neuron, 76*, 130—141.

Sherman, S. M. (2001). Tonic and burst firing: dual modes of thalamocortical relay. *TINS, 24*(2), 122—126.

Sherman, S. M., & Guillery, R. W. (2001). *Exploring the thalamus*. California, USA: Academic Press.

Shine, J. M., Halliday, G. M., Gilat, M., Matar, E., Bolitho, S. J., Carlos, M., & Lewis, S. J. (2014). The role of dysfunctional attentional control networks in visual misperceptions in Parkinson's disease. *Human Brain Mapping, 35*(5), 2206—2219.

Sincich, L. C., Park, K. F., Wohlgemuth, M. J., & Horton, J. C. (2004). Bypassing V1: a direct geniculate input to area MT. *Nature Neuroscience, 7*(10), 1123—1128.

St Louis, E. K., McCarter, S. J., Boeve, B. F., Silber, M. H., Kantarci, K., Benarroch, E. E., et al. (2014). Lesional REM sleep behavior disorder localizes to the dorsomedial pons. *Neurology, 83*, 1871—1873.

Stebbins, G. T., Goetz, C. G., Carrillo, M. C., Bangen, K. J., Turner, D. A., Glover, G. H., et al. (2004). Altered cortical visual processing in PD with hallucinations. *Neurology, 63*, 1409—1416.

Tehovnik, E. J., Sommer, M. A., Chou, I. H., Slocum, W. M., & Schiller, P. H. (2000). Eye fields in the frontal lobes of primates. *Brain Research Reviews, 32*, 413—448.

Trapp, S., & Bar, M. (2015). Prediction, context, and competition in visual recognition. *Annals of the New York Academy of Sciences, 1339*, 190—198.

Triantafyllou, C., Polimeni, J. R., & Wald, L. L. (2011). Physiological noise and signal-to-noise ratio in fMRI with multi-channel array coils. *NeuroImage, 55*(2), 597—606.

Uchiyama, M., Nishio, Y., Yokoi, K., Hirayama, K., Imamura, T., Shimomura, T., et al. (2012). Pareidolias: complex visual

illusions in dementia with Lewy bodies. *Brain, 135*(Pt 8), 2458–2469.

Van Dijk, K. R., Hedden, T., Venkataraman, A., Evans, K. C., Lazar, S. W., & Buckner, R. L. (2010). Intrinsic functional connectivity as a tool for human connectomics: theory, properties, and optimization. *Journal of Neurophysiology, 103*(1), 297–321.

Vetrugno, R., Vella, A., Mascalchi, M., Alessandria, M., D'Angelo, R., Gallassi, R., et al. (2009). Peduncular hallucinosis: a polysomnographic and spect study of a patient and efficacy of serotonergic therapy. *Sleep Medicine, 10*(10), 1158–1160.

Vignal, J. P., Chauvel, P., & Halgren, E. (2000). Localised face processing by the human prefrontal cortex: stimulation-evoked halluincations of faces. *Cognive Neuropsyhology, 17*, 281–291.

Walz, J. M., Goldman, R. I., Carapezza, M., Muraskin, J., Brown, T. R., & Sajda, P. (2013). Simultaneous EEG-fMRI reveals temporal evolution of coupling between supramodal cortical attention networks and the brainstem. *Journal of Neuroscience, 33*(49), 19212–19222.

West, C. J. (1962). *Hallucinations* (pp. 43–46). New York: Greene & Stratton.

Whitfield-Gabrieli, S., & Nieto-Castanon, A. (2012). Conn: a functional connectivity toolbox for correlated and anticorrelated networks. *Brain Connectivity, 2*, 125–141.

Zhang, Q., Wang, D., Qin, W., Li, Q., Chen, B., Zhang, Y., et al. (2012). Altered resting-state brain activity in obstructive sleep apnea. *Sleep, 36*(5), 651–659.